

CNRS

Centre National de la Recherche Scientifique

INFN

Istituto Nazionale di Fisica Nucleare

**The thermal noise of the Virgo+ and Virgo Advanced
Last Stage Suspension (The PPP effect).**

F. Piergiovanni, M. Punturo and P. Puppo

VIR-015A-09

Issue:1
Date: 14 April, 2009

VIRGO *Traversa H di via Macerata-56021 S. Stefano a Macerata, Cascina (PI), Italy.
Secretariat: Telephone.(39) 050 752 521 * FAX.(39) 050 752 550 * e-mail manuela@virgo.infn.it

Introduction

The calculation of the Virgo sensitivity curve is usually performed by including just the thermal noise of the mirror pendulum with the assumption that the effect of the other masses like the marionette and the reaction mass is negligible in the bandwidth of interest. However, this assumption is valid if the marionette mass is higher than those ones of the mirror and the reaction mass because its recoil is negligible under these hypotheses. These conditions can be less valid in the case of the Virgo Advanced suspension in which the mirror suspension losses are very low and the masses of the marionette and the mirror are likely to be comparable. For this reason, we have computed the contribution to the pendulum thermal noise of the whole Virgo last stage suspensions, without any assumption on the masses amounts.

This note is meant to give an overview of the calculations performed by the three authors on the mirror last stage suspension thermal noise. So, in the following you'll find the three different approaches that will lead to results which are in full agreement.

The paper is divided into three main sections (1, 2, 3), each of them referring to a different approach. For this reason the notations used can be slightly different but consistent within the same section.

1. Direct application of the Fluctuation-Dissipation theorem and matrix approach

The computation is an extension of what made by M.Punturo and F.Travasso in the Virgo internal note (Punturo M. 2003).

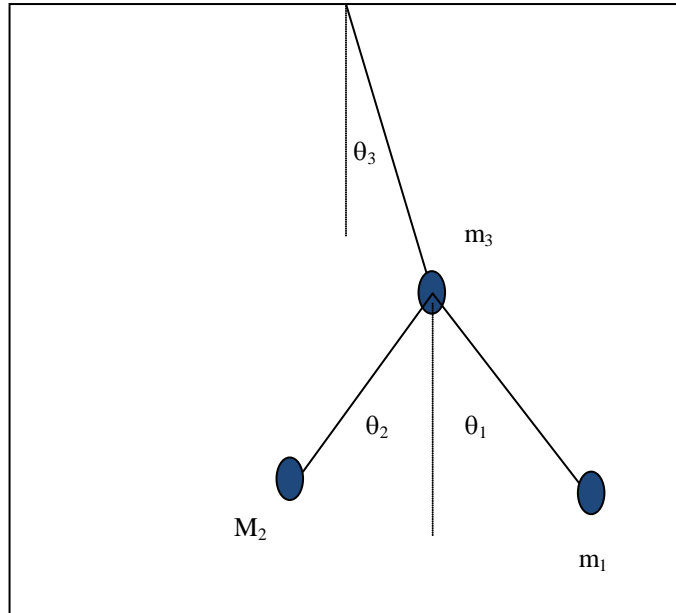
1.1. Evaluation of the Lagrangian of the system

In this section the following indices are used:

- 1) Mirror
- 2) Reference Mass
- 3) Marionette

The coordinates adopted are the Virgo standard:

- Horizontal axis, orthogonal to the beam: x
- Horizontal axis, parallel to the beam: z
- Vertical axis: y



It is well known that the equations of the motion of a mechanical system could be obtained through the Euler-Lagrange equations:

$$(1) \quad \frac{d}{dt} \left(\frac{\partial \mathcal{L}}{\partial \dot{q}_j} \right) - \frac{\partial \mathcal{L}}{\partial q_j} = 0$$

where \mathcal{L} is the Lagrangian of the system defined by:

$$(2) \quad \mathcal{L} = T - V$$

being T the kinetic energy of the system and V the potential energy.

In our case, the displacements of interest (on which we compute the thermal noises) are:

$$(3) \quad \left. \begin{aligned} z_1 &= L_1\theta_1 + L_3\theta_3 \\ z_2 &= L_2\theta_2 + L_3\theta_3 \\ z_3 &= L_3\theta_3 \end{aligned} \right\} \Rightarrow \begin{cases} L_1\theta_1 = z_1 - z_3 \\ L_2\theta_2 = z_2 - z_3 \\ L_3\theta_3 = z_3 \end{cases}$$

Hence, the velocity of the mirror is given by:

$$(4) \quad \begin{aligned} v_z &= \dot{z}_1 = L_1\dot{\theta}_1 + L_3\dot{\theta}_3 \\ v_y &= \dot{y}_1 = L_1\theta_1\dot{\theta}_1 + L_3\theta_3\dot{\theta}_3 \end{aligned}$$

The second term is negligible since it introduces just 3rd order terms. The kinetic energy of the mirror is then:

$$(5) \quad T_1 = \frac{1}{2}m_1 \left(L_1\dot{\theta}_1 + L_3\dot{\theta}_3 \right)^2$$

The reference mass is perfectly symmetric, swapping the index $1 \leftrightarrow 2$. The Marionette kinetic energy is:

$$(6) \quad T_3 = \frac{1}{2}m_3 \left(L_3\dot{\theta}_3 \right)^2$$

Since we want to introduce the thermal noise, we cannot consider the forces conservative and then we cannot introduce a simple gravitational potential energy. It can be demonstrated (see text books like (Goldstein s.d.)) that (1) is still valid if we replace the potential energy by a “generalized potential” $U(q_j, \dot{q}_j)$ such as the generalized forces F_{gj} could be written:

$$(7) \quad F_{gj} = -\frac{\partial U}{\partial q_j} + \frac{d}{dt} \left(\frac{\partial U}{\partial \dot{q}_j} \right)$$

In the pendulum case this requirement is satisfied. In fact the restoring force is given mainly by the gravitation, and the conservative potential energy is simply $m_j g \Delta y_j$, and partially by the elastic reaction of the bended suspension wire. The gravitational contribution to the generalized potential is:

$$(8) \quad \left. \begin{aligned} U_g|_{j=1,2} &= m_j g \left(\frac{L_j\theta_j^2}{2} + \frac{L_3\theta_3^2}{2} \right) = \frac{1}{2}m_j \left(\omega_{pj}^2 L_j^2 \theta_j^2 + \omega_{p3}^2 L_3^2 \theta_3^2 \right) = \frac{1}{2}m_j \left(\omega_{pj}^2 z_j^2 + \omega_{p3}^2 z_3^2 \right) \\ U_g|_3 &= m_3 g \frac{L_3\theta_3^2}{2} = \frac{1}{2}m_3 \omega_{p3}^2 L_3^2 \theta_3^2 = \frac{1}{2}m_3 \omega_{p3}^2 z_3^2 \end{aligned} \right\} \Rightarrow U_g = \sum_{j=1}^3 U_g|_j$$

where $\omega_p = \sqrt{g/L}$ is the angular frequency of the pendulum.

The elastic constant of the bended suspension wire is given by:

$$(9) \quad k_j = \frac{n_j b_j \sqrt{\Lambda_j Y_j I_{2j}}}{2L_j^2} = \begin{cases} \frac{b_j \sqrt{n_j (m_j g) Y_j I_{2j}}}{2L_j^2} & ; j = 1, 2 \\ \frac{b_j \sqrt{n_j (M_T g) Y_j I_{2j}}}{2L_j^2} & ; j = 3 \end{cases}$$

Where n_j is the number of suspension wires (usually, in Virgo and advanced Virgo, $n_1=n_2=4$, $n_3=1$), b_j is the number of flexural points ($n_j=2$), $\Lambda=mg/n$ is the tension of each suspension wire ($M_T=m_1+m_2+m_3$), Y_j is the Young modulus of the suspension wires, $I_2 = \frac{\pi}{4} r^4$ is the cross-section momentum (r =radius of the suspension wire, supposed cylindrical).

To introduce the dissipation in the wire, according to the so-called structural model, it is enough to apply the substitution:

$$(10) \quad k_j \Rightarrow k_j (1 + i\varphi_{s_j})$$

The generalized elastic potential, for each bended pendulum, is

$$(11) \quad U_e|_j = \frac{1}{2} k_j z_j^2 = \frac{1}{2} m_j \omega_{w_j}^2 z_j^2 = \frac{1}{2} m_j \omega_{w_j}^2 L_j^2 \theta_j^2$$

where, neglecting for simplicity the index j :

$$(12) \quad \omega_w^2 = \frac{k}{m} = \frac{b \cdot g}{2L^2} \sqrt{\frac{n Y I_2}{mg}} = \omega_p^2 \frac{b}{2L} \sqrt{\frac{n Y I_2}{mg}} = \omega_p^2 D$$

Where D is called dilution factor and $m = m_1, m_2, M_T$.

Comparing (11) with (8), it is evident that, for each bended pendulum we should consider a gravitational and an elastic generalized potential that could be written in a more compact shape if we introduce the effective oscillation angular frequency:

$$(13) \quad \omega_j^2 = \omega_{p_j}^2 + \omega_{w_j}^2 = \omega_{p_j}^2 \left[(1 + D_j) + iD_j \varphi_j \right]$$

Since D is usually small (of the order of $10^{-2} - 10^{-3}$), the real part of the pendulum frequency is slightly affected by the elastic contribution, and the internal losses of the suspension wires are down-scaled by the pendulum dilution factor. Adopting equation (13), the generalized elastic and gravitational potential is:

$$(14) \quad \left. \begin{aligned} U_g|_{j=1,2} &= \frac{1}{2} m_j (\omega_j^2 L_j^2 \theta_j^2 + \omega_3^2 L_3^2 \theta_3^2) = \frac{1}{2} m_j (\omega_j^2 z_j^2 + \omega_3^2 z_3^2) \\ U_{ge}|_3 &= \frac{1}{2} m_3 \omega_3^2 L_3^2 \theta_3^2 = \frac{1}{2} m_3 \omega_3^2 z_3^2 \end{aligned} \right\} \Rightarrow U_{ge} = \sum_{j=1}^3 U_{ge}|_j$$

The new Lagrangian, including the structural dissipation is, then:

$$(15) \quad \mathcal{L} = T - U_{ge} = \frac{1}{2} m_1 (L_1 \dot{\theta}_1 + L_3 \dot{\theta}_3)^2 + \frac{1}{2} m_2 (L_2 \dot{\theta}_2 + L_3 \dot{\theta}_3)^2 + \frac{1}{2} m_3 (L_3 \dot{\theta}_3)^2 - \frac{1}{2} m_1 (\omega_1^2 L_1^2 \theta_1^2 + \omega_3^2 L_3^2 \theta_3^2) - \frac{1}{2} m_2 (\omega_2^2 L_2^2 \theta_2^2 + \omega_3^2 L_3^2 \theta_3^2) - \frac{1}{2} m_3 \omega_3^2 L_3^2 \theta_3^2$$

The structural model is not appropriate to describe the frictional damping processes that could occur on the payload (like magnetic dissipation, residual gas damping, and excess losses in the mechanics, ...). For this reason we need to introduce a viscous force given by $F=-m\gamma v$, where v is the velocity of the body and $\gamma_j = \text{Re}(\omega_j)/Q_j$ (Q is the mechanical Q of the damping process). This viscous force could be derived by a dissipation Rayleigh potential function:

$$(16) \quad \Psi = \frac{1}{2} \sum_{j=1}^3 m_j \gamma_j (L_j \dot{\theta}_j)^2$$

Note that the (17) is appropriate to describe viscous dissipation processes related to the velocities of the bodies respect their own suspension point, but not to describe global viscous dumping, like the residual gas, where the composition of the velocities (i.e. v_1+v_3) should be considered.

Introducing this potential function, the Lagrangian equations become:

$$(17) \quad \frac{d}{dt} \left(\frac{\partial \mathcal{L}}{\partial \dot{q}_j} \right) - \frac{\partial \mathcal{L}}{\partial q_j} + \frac{\partial \Psi}{\partial \dot{q}_j} = 0$$

Solving these equations we obtain the system of motion equation:

$$(18) \quad \begin{cases} m_1 L_1 \{ L_1 \ddot{\theta}_1 + L_3 \ddot{\theta}_3 + \omega_1^2 L_1 \theta_1 + \gamma_1 L_1 \dot{\theta}_1 \} = 0 \\ m_2 L_2 \{ L_2 \ddot{\theta}_2 + L_3 \ddot{\theta}_3 + \omega_2^2 L_2 \theta_2 + \gamma_2 L_2 \dot{\theta}_2 \} = 0 \\ M_T L_3 \{ \mu_1 (L_1 \ddot{\theta}_1) + \mu_2 (L_2 \ddot{\theta}_2) + (L_3 \ddot{\theta}_3) + \omega_3^2 (L_3 \theta_3) + \mu_3 \gamma_3 (L_3 \dot{\theta}_3) \} = 0 \end{cases}$$

Where

$$(19) \quad M_T = m_1 + m_2 + m_3 \quad ; \quad \mu_j = \frac{m_j}{M_T}$$

To evaluate the thermal noise If we consider the stochastic thermal noise forces F_j , that are applied at each pendulum body, the generalized stochastic thermal forces F_{gj} are:

$$(20) \quad F_{gj} \equiv \sum_{i=1}^3 F_i \cdot \frac{\partial z_i}{\partial q_j} = \begin{cases} F_1 \cdot L_1 \\ F_2 \cdot L_2 \\ (F_1 + F_2 + F_3) \cdot L_3 \end{cases}$$

and (17) becomes

$$(21) \quad \frac{d}{dt} \left(\frac{\partial \ell}{\partial \dot{q}_j} \right) - \frac{\partial \ell}{\partial q_j} + \frac{\partial \Psi}{\partial \dot{q}_j} = F_{gj}$$

Considering the thermal driving force, the equations are then:

$$(22) \quad \begin{cases} L_1 \ddot{\theta}_1 + L_3 \ddot{\theta}_3 + \omega_1^2 L_1 \theta_1 + \gamma_1 L_1 \dot{\theta}_1 = \frac{F_1}{m_1} \\ L_2 \ddot{\theta}_2 + L_3 \ddot{\theta}_3 + \omega_2^2 L_2 \theta_2 + \gamma_2 L_2 \dot{\theta}_2 = \frac{F_2}{m_2} \\ \mu_1 (L_1 \ddot{\theta}_1) + \mu_2 (L_2 \ddot{\theta}_2) + (L_3 \ddot{\theta}_3) + \omega_3^2 (L_3 \theta_3) + \mu_3 \gamma_3 (L_3 \dot{\theta}_3) = \frac{F_1 + F_2 + F_3}{M_T} \end{cases}$$

Let sum at the third equation the first one multiplied by $-\mu_1$ and the second one by $-\mu_2$:

$$(23) \quad \begin{cases} L_1 \ddot{\theta}_1 + L_3 \ddot{\theta}_3 + \omega_1^2 L_1 \theta_1 + \gamma_1 L_1 \dot{\theta}_1 = \frac{F_1}{m_1} \\ L_2 \ddot{\theta}_2 + L_3 \ddot{\theta}_3 + \omega_2^2 L_2 \theta_2 + \gamma_2 L_2 \dot{\theta}_2 = \frac{F_2}{m_2} \\ L_3 \ddot{\theta}_3 - \frac{\mu_1}{\mu_3} \omega_1^2 L_1 \theta_1 - \frac{\mu_2}{\mu_3} \omega_2^2 L_2 \theta_2 + \frac{1}{\mu_3} \omega_3^2 (L_3 \theta_3) + \gamma_3 L_3 \dot{\theta}_3 - \frac{\mu_1}{\mu_3} \gamma_1 L_1 \dot{\theta}_1 - \frac{\mu_2}{\mu_3} \gamma_2 L_2 \dot{\theta}_2 = \frac{F_3}{m_3} \end{cases}$$

Or in displacement:

$$(24) \begin{cases} \ddot{z}_1 + \omega_1^2 z_1 - \omega_1^2 z_3 + \gamma_1 \dot{z}_1 - \gamma_1 \dot{z}_3 = \frac{F_1}{m_1} \\ \ddot{z}_2 + \omega_2^2 z_2 - \omega_2^2 z_3 + \gamma_2 \dot{z}_2 - \gamma_2 \dot{z}_3 = \frac{F_2}{m_2} \\ \ddot{z}_3 - \frac{\mu_1}{\mu_3} \omega_1^2 z_1 - \frac{\mu_2}{\mu_3} \omega_2^2 z_2 + \frac{\omega_3^2 + \mu_1 \omega_1^2 + \mu_2 \omega_2^2}{\mu_3} z_3 - \frac{\mu_1}{\mu_3} \gamma_1 \dot{z}_1 - \frac{\mu_2}{\mu_3} \gamma_2 \dot{z}_2 + \frac{\mu_1 \gamma_1 + \mu_2 \gamma_2 + \mu_3 \gamma_3}{\mu_3} \dot{z}_3 = \frac{F_3}{m_3} \end{cases}$$

1.2. Using matrix formalism

The equation (24) can be expressed in matrix formalism:

$$(25) \quad I \frac{d^2}{dt^2} X + \Gamma \frac{d}{dt} X + \Omega \cdot X = M^{-1} F$$

Where I is the identity matrix:

$$(26) \quad I = \begin{pmatrix} 1 & 0 & 0 \\ 0 & 1 & 0 \\ 0 & 0 & 1 \end{pmatrix}$$

Γ is the matrix of the damping coefficients:

$$(27) \quad \Gamma = \begin{pmatrix} \gamma_1 & 0 & -\gamma_1 \\ 0 & \gamma_2 & -\gamma_2 \\ -\frac{\mu_1}{\mu_3} \gamma_1 & -\frac{\mu_2}{\mu_3} \gamma_2 & \frac{\mu_1 \gamma_1 + \mu_2 \gamma_2 + \mu_3 \gamma_3}{\mu_3} \end{pmatrix}$$

Ω is the matrix of the pendulum frequencies

$$(28) \quad \Omega = \begin{pmatrix} \omega_1^2 & 0 & -\omega_1^2 \\ 0 & \omega_2^2 & -\omega_2^2 \\ -\frac{\mu_1}{\mu_3} \omega_1^2 & -\frac{\mu_2}{\mu_3} \omega_2^2 & \frac{\mu_1 \omega_1^2 + \mu_2 \omega_2^2 + \omega_3^2}{\mu_3} \end{pmatrix}$$


M is the masses matrix:

$$(29) \quad M = \begin{pmatrix} m_1 & 0 & 0 \\ 0 & m_2 & 0 \\ 0 & 0 & m_3 \end{pmatrix}$$

X is the column vector of the displacements z_j , F is the column vector of the thermal stochastic forces F_j , and d/dt are the derivative operators.

In the Fourier transform, (25) becomes:

$$(30) \quad \begin{aligned} (\Omega - \omega^2 I + i\omega \cdot \Gamma) \cdot \tilde{X} &= M^{-1} \tilde{F} \Rightarrow \\ \tilde{X} &= (\Omega - \omega^2 I + i\omega \cdot \Gamma)^{-1} M^{-1} \tilde{F} = \left[M \cdot (\Omega - \omega^2 I + i\omega \cdot \Gamma) \right]^{-1} \cdot \tilde{F} \end{aligned}$$

	The thermal noise of the Virgo+ and Virgo Advanced Last Stage Suspension (The PPP effect).	DOC: Vir-015A-09 Issue: 1 Date: April 2009
---	---	--

By definition, the transfer function H is:

$$(31) \quad \tilde{X} \equiv H \cdot \tilde{F} \Rightarrow H = \left[M \cdot (\Omega - \omega^2 I + i\omega \cdot \Gamma) \right]^{-1}$$

The mechanical impedance of the system is

$$(32) \quad \tilde{F} \equiv Z \cdot \dot{\tilde{X}} \Rightarrow Z = \frac{1}{i\omega} H^{-1} = \frac{1}{i\omega} \left[M \cdot (\Omega - \omega^2 I + i\omega \cdot \Gamma) \right]$$

1.3. Pendulum thermal noise

Finally, thanks to the Fluctuation-Dissipation Theorem (FDT), the power spectrum of the thermal noise displacement of the mirror (index j=1) is given by:

$$(33) \quad \langle x_1 \rangle^2 = \frac{4k_B T}{\omega^2} \Re \left\{ (Z^{-1})_{11} \right\} = \frac{4k_B T}{\omega^2} \Re \left\{ \left[\left(\frac{1}{i\omega} \cdot M \cdot (\Omega - \omega^2 I + i\omega \cdot \Gamma) \right)^{-1} \right]_{11} \right\}$$

1.4. Thermoelastic dissipation

For sake of completeness, we should report that an important dissipation in the suspension wires is the thermo-elastic dissipation:

$$(34) \quad \varphi_{th}(\omega) = \left(\alpha - \beta_E \frac{\Lambda}{Y \cdot S} \right)^2 \frac{Y \cdot T}{C_V} \frac{\omega \tau}{1 + (\omega \tau)^2}$$

Usually this dissipation is inserted in the loss angle definition:

$$(35) \quad \begin{aligned} \varphi(\omega) &= \varphi_{mat} + \varphi_{surf} + \varphi_{th}(\omega) \\ \varphi_{surf} &= \varphi_{mat} \left(\xi \frac{d_s}{V/S} \right) \end{aligned}$$

where ϕ_{mat} is the material intrinsic loss angle and ϕ_{surf} is the excess loss due to the wire surface. The thermoelastic dissipation depends by the velocity of the oscillation (ω) and then the previous mathematical description is still valid since we can introduce a “generalized potential” $U(q_j, \dot{q}_j)$.

1.5. Vertical mode

The vertical oscillation of the payload can be computed applying equation (21) to the vertical Lagrangian and to the vertical viscous damping forces. The generalized coordinates are the vertical quotes of the three bodies; hence:

$$(36) \quad \begin{aligned} \mathcal{L}_v = T_v - U_{ve} &= \frac{1}{2} m_1 \dot{y}_1^2 + \frac{1}{2} m_2 \dot{y}_2^2 + \frac{1}{2} m_3 \dot{y}_3^2 - \frac{1}{2} k_1 (y_1 - y_3)^2 - \frac{1}{2} k_2 (y_2 - y_3)^2 - \frac{1}{2} k_3 y_3^2 \\ &= \frac{1}{2} m_1 \dot{y}_1^2 + \frac{1}{2} m_2 \dot{y}_2^2 + \frac{1}{2} m_3 \dot{y}_3^2 - \frac{1}{2} m_1 \omega_{v1}^2 (y_1 - y_3)^2 - \frac{1}{2} m_2 \omega_{v2}^2 (y_2 - y_3)^2 - \frac{1}{2} M_T \omega_{v3}^2 y_3^2 \end{aligned}$$

Where

$$(37) \quad \omega_{vj}^2 = \begin{cases} \frac{k_j}{m_j} & ; \quad j = 1, 2 \\ (2\pi \cdot 0.4)^2 & ; \quad j = 3 \end{cases} \quad k_j = n_j Y_j \frac{\pi r_j^2}{L_j}$$

The vertical frequency of the marionette is dominated by the softness of the magnetic anti-spring suspension system (0.4 Hz of vertical frequency measured with the suspended system) so the reaction constant can be written as $k_3 = (2\pi \cdot 0.4)^2 \cdot M_T$.

Considering only viscous terms generated by the reciprocal motion of the masses, the Rayleigh potential is:

$$(38) \quad \Psi_v = \frac{1}{2} m_1 \gamma_1 (\dot{y}_1 - \dot{y}_3)^2 + \frac{1}{2} m_2 \gamma_2 (\dot{y}_2 - \dot{y}_3)^2 + \frac{1}{2} m_3 \gamma_3 \dot{y}_3^2$$

where the γ_i could be numerically different from the horizontal ones.

The system of motion equation is:

$$(39) \quad \begin{cases} \ddot{y}_1 + \omega_{v1}^2 y_1 - \omega_{v1}^2 y_3 + \gamma_1 \dot{y}_1 - \gamma_1 \dot{y}_3 = \frac{F_1}{m_1} \\ \ddot{y}_2 + \omega_{v2}^2 y_2 - \omega_{v2}^2 y_3 + \gamma_2 \dot{y}_2 - \gamma_2 \dot{y}_3 = \frac{F_2}{m_2} \\ \ddot{y}_3 - \frac{m_1}{m_3} \omega_{v1}^2 y_1 - \frac{m_2}{m_3} \omega_{v2}^2 y_2 + \frac{m_1 \omega_{v1}^2 + m_2 \omega_{v2}^2 + M_T \omega_{v3}^2}{m_3} y_3 + \frac{m_1}{m_3} \gamma_1 \dot{y}_1 + \frac{m_2}{m_3} \gamma_2 \dot{y}_2 + \frac{m_3 \gamma_3 - m_1 \gamma_1 - m_2 \gamma_2}{m_3} \dot{y}_3 = \frac{F_3}{m_3} \end{cases}$$

The matrix formalism introduced in (25) is fully valid and then the vertical thermal noise is still described by the(33), where the matrices are:

$$(40) \quad \Gamma_v = \begin{pmatrix} \gamma_1 & 0 & -\gamma_1 \\ 0 & \gamma_2 & -\gamma_2 \\ \frac{\mu_1}{\mu_3} \gamma_1 & \frac{\mu_2}{\mu_3} \gamma_2 & \frac{\mu_3 \gamma_3 - \mu_1 \gamma_1 - \mu_2 \gamma_2}{\mu_3} \end{pmatrix} ; \quad \Omega_v = \begin{pmatrix} \omega_{v1}^2 & 0 & -\omega_{v1}^2 \\ 0 & \omega_{v2}^2 & -\omega_{v2}^2 \\ -\frac{\mu_1}{\mu_3} \omega_{v1}^2 & -\frac{\mu_2}{\mu_3} \omega_{v2}^2 & \frac{\mu_1 \omega_{v1}^2 + \mu_2 \omega_{v2}^2 + \omega_{v3}^2}{\mu_3} \end{pmatrix}$$

Inserting the matrices, reported in equation (40), inside the equation (33) the contribution of the vertical fluctuation to the thermal noise seen by the interferometer could be computed, using the appropriate vertical-to-horizontal coupling angle.

2. Thermal noise calculation including the elastic stiffness for the mirror suspension fibres.

The elastic constant of the suspension wire is negligible compared to the gravitational one, in the low frequency range. But approaching the violin modes frequencies, the elastic energy increases so that the elastic behaviour of the bended fibre must be taken into account. To do this, it is necessary to solve the elastic equation for a slightly deflected rod stretched by a tension T:

$$(41) \quad -EIx^{(iv)}(y) + Tx''(y) = \rho S \ddot{x}(y)$$

For harmonic excitation, the Fourier transform leads to:

$$(42) \quad EIX^{(iv)}(y) - TX''(y) - \rho S \omega^2 X(y) = 0$$

where E is the Young modulus, I the moment of inertia, ρ the density, S the cross section and X the deflection. The derivatives are calculated with respect to the y coordinates along the rod axis. For cylindrical fibres an analytical solution can be found:

$$(43) \quad X(y) = Ae^{-\lambda y} + Be^{-\lambda(L-y)} + C \cos(py) + D \sin(py)$$

where:

$$(44) \quad \lambda = \sqrt{\frac{T + \sqrt{T^2 + 4EI\rho S \omega^2}}{2EI}}$$

$$(45) \quad p = \sqrt{\frac{-T + \sqrt{T^2 + 4EI\rho S \omega^2}}{2EI}}$$

Boundary conditions fix the values of the constants A,B,C,D:

$$(46) \quad X(0) = 0; \quad X'(0) = 0; \quad X(L) = \delta; \quad X'(L) = 0$$

The first and the second conditions come from the clamping of the fibre at one end, the third says that the other end is shifted horizontally by a length δ and the last is due to the 4 fibres mirror holding configuration that depresses the θ_x tilt. The force at the end of the fibre can be obtained by:

$$(47) \quad F = -EIX'''(L)$$

The force results proportional to the shift δ , thus it is possible to define an effective frequency dependent stiffness constant $k = \frac{F}{\delta}$. The complete expression for k is:

$$(48) \quad k(\omega) = \frac{4EI\lambda p (\lambda^3 \cos(pL) + \lambda^2 p \sin(pL) + \lambda p^2 \cos(pL) + p^3 \sin(pL))}{(\lambda^2 - p^2) \sin(pL) - 2\lambda p \cos(pL)}$$

This stiffness constant is used to calculate the angular frequency $\omega_1 = \sqrt{k(\omega) / m_1}$ and replaces the corresponding quantity defined in the equations (13). The internal damping can be considered adding an imaginary part to the Young modulus $E = E_0(1 + i\phi_{\text{int}})$ where E_0 is the Young modulus of the material and ϕ_{int} is the sum of bulk, surface and thermoelastic contributions.

Up to now this more accurate calculation of the stiffness was only performed for mirror suspension fibres. But in the next future same approach should be extended to the RM and Marionette wires and a more realistic lagrangian must be written taking into account in particular the marionette tilts.

2.1. Optimized fibres

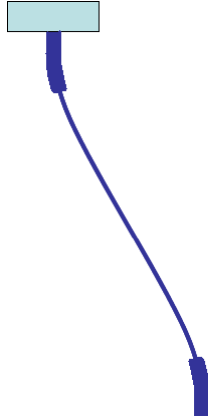
Equation (34) shows that a complete cancellation of the thermoelastic contribution is possible choosing the fibre diameter according to the load tension. For a mirror mass of 40 kg the resulting diameter is about 820 μ m.

From complete computation results that thermal noise is minimized with a diameter of about 800 μ m.

On the other hand, for a 40kg mass mirror, the safe working stress is reached using four 400 μ m diameter suspension fibres. Thinner fibres push down vertical mode frequency and shift the violin modes at higher frequencies.

In principle is possible to join the benefits of thinner and thicker fibres.

The so called “optimized fibres” have two heads at the ends, with a length of a few cm’s and a 800 μ m diameter, and a



central part with a 400 μ m diameter.

At low energy, if thicker heads are longer than the bending length ($1/\lambda$ equation (45)) the whole elastic energy is stored in these regions. Hence dissipations are confined in the 800 μ m diameter region and the thermal noise is minimized. On the other hand the bouncing and the first violin modes will be dominated by the thinner region of the fibre and the frequencies for these modes will be very similar to those of cylindrical fibres with 400 μ m in diameter.

If sharp diameter transitions are considered, an analytic solution of the elastic equation can be found also for optimized fibres.

The elastic equation (42) becomes:

$$(49) \quad EI_j X^{(iv)}(y) - TX''(y) - \rho S_j \omega^2 X(y) = 0$$

where $j=1,2,3$ respectively for the first head, the central part and the last head.

One solution can be written for each part of the fibre:

$$(50) \quad X_j = A_j e^{-\lambda_j y} + B_j e^{-\lambda_j(L_j-y)} + C_j \cos(p_j y) + D_j \sin(p_j y)$$

$$j = 1, 2, 3$$


The twelve constants (A_j, B_j, C_j, D_j) can be found from the 4 boundary conditions (46) and from the joining conditions for the function X and the derivative X' in the diameter discontinuity points.

Thus it is possible to find the stiffness constants k (as explained in the previous section) and the elastic energy distribution:

$$(51) \quad u_{elastic}(y) = \frac{1}{2} EI (X'')^2$$

$$U_{elastic} = \int_0^L u_{elastic}(y) dy$$

Each diameter dependent loss angle (surface and thermoelastic contributions) can be weighted with the distribution energy:

	The thermal noise of the Virgo+ and Virgo Advanced Last Stage Suspension (The PPP effect).	DOC: Vir-015A-09 Issue: 1 Date: April 2009
---	---	--

(52)
$$\phi = \frac{\int_0^L \phi(y) u_{elastic}(y) dy}{U_{elastic}}$$

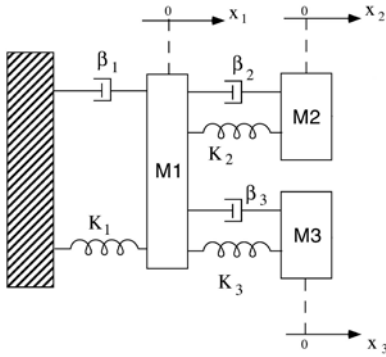
Bulk contribution, that is obviously diameter independent, can be added to obtain the internal total loss angle. No viscous dissipation is considered for the mirror suspension fibres. So it is possible to write the Young modulus as in equation (45), and the thermal noise can be computed by replacing the stiffness constant k_1 in the lagrangian of the system with the value obtained from the expression

(53)
$$k = -\frac{EI_3 X_3^{iii}(L_3)}{\delta}$$

3. The normal modes study

The last stage suspension system is schematized as a branched combination of three harmonic oscillators (see Figure

3-1) where m_1 , m_2 and m_3 are the masses of the marionette, the mirror and the reaction mass respectively. So the following indices are used:



- 1) Marionette
- 2) Mirror
- 3) Reaction Mass

The mechanical study of such a system was already presented in the paper (A. Bernardini 1999), where their frequencies were calculated.

3-1 Branched System

The Lagrangian and the dissipative function of the system are:

$$\mathcal{L} = \frac{1}{2} m_1 \dot{x}_1^2 + \frac{1}{2} m_2 \dot{x}_2^2 + \frac{1}{2} m_3 \dot{x}_3^2 - \frac{1}{2} m_1 \omega_1^2 x_1^2 - \frac{1}{2} m_2 \omega_2^2 (x_1 - x_2)^2 - \frac{1}{2} m_3 \omega_3^2 (x_1 - x_3)^2$$

$$E_d = \frac{1}{2} m_1 \frac{\omega_1}{Q_1} \dot{x}_1^2 - \frac{1}{2} m_2 \frac{\omega_2}{Q_2} (\dot{x}_1 - \dot{x}_2)^2 - \frac{1}{2} m_3 \frac{\omega_3}{Q_3} (\dot{x}_1 - \dot{x}_3)^2$$
(54)

Where $Q_i, i = 1, \dots, 3$ are the mechanical quality factors of the uncoupled harmonic oscillators.

The equation of motion can be obtained by the Lagrange equations:

$$\frac{d}{dt} \frac{\partial \mathcal{L}}{\partial \dot{x}_i} = \frac{\partial \mathcal{L}}{\partial x_i} - \frac{\partial E_d}{\partial \dot{x}_i}$$
(56)

$$\left\{ \begin{array}{l} \ddot{x}_1 + \frac{\omega_1}{Q_1} \dot{x}_1 + \mu_{21} \frac{\omega_2}{Q_2} (\dot{x}_1 - \dot{x}_2) + \omega_1^2 x_1 + \\ \quad + \mu_{21} \omega_2^2 (x_1 - x_2) + \mu_{31} \frac{\omega_3}{Q_3} (\dot{x}_1 - \dot{x}_3) + \mu_{31} \omega_3^2 (x_1 - x_3) = f_{thI} / m_1 \\ \ddot{x}_2 + \frac{\omega_2}{Q_2} (\dot{x}_1 - \dot{x}_2) + \omega_2^2 (x_1 - x_2) = f_{thII} / m_2 \\ \ddot{x}_3 + \frac{\omega_3}{Q_3} (\dot{x}_1 - \dot{x}_3) + \omega_3^2 (x_1 - x_3) = f_{thIII} / m_3 \end{array} \right.$$
(57)

where $\mu_{21} = m_2 / m_1$; $\mu_{31} = m_3 / m_1$ are mass ratios. The stochastic thermal generalized forces in the right side can be consistently related to the uncoupled term as:

$$f_{thI} = f_{th1} - f_{th2} - f_{th3}; f_{thII} = f_{th2}; f_{thIII} = f_{th3}$$
(58)

If we take the Fourier transform of this system we get:

$$\hat{D} \begin{pmatrix} X_1 \\ X_2 \\ X_3 \end{pmatrix} = \begin{pmatrix} F_{thI} / m_1 \\ F_{thII} / m_2 \\ F_{thIII} / m_3 \end{pmatrix}$$
(59)

Where the matrix \hat{D} can be written as:

$$(60) \quad \hat{D} = \begin{pmatrix} -\omega^2 + \omega_1^2 + \mu_{21}\omega_2^2 + \mu_{31}\omega_3^2 + i\omega\left(\frac{\omega_1}{Q_1} + \mu_{21}\frac{\omega_2}{Q_2} + \mu_{31}\frac{\omega_3}{Q_3}\right) & -\mu_{21}\omega_2^2 - i\omega\left(\mu_{21}\frac{\omega_2}{Q_2}\right) & -\mu_{31}\omega_3^2 - i\omega\left(\mu_{31}\frac{\omega_3}{Q_3}\right) \\ -\omega_2^2 - i\omega\left(\frac{\omega_2}{Q_2}\right) & -\omega^2 + \omega_2^2 + i\omega\left(\frac{\omega_2}{Q_2}\right) & 0 \\ -\omega_3^2 - i\omega\left(\frac{\omega_3}{Q_3}\right) & 0 & -\omega^2 + \omega_3^2 + i\omega\left(\frac{\omega_3}{Q_3}\right) \end{pmatrix}$$

or, in terms of the impedance matrix:

$$(61) \quad \hat{Z} \begin{pmatrix} X_1 \\ X_2 \\ X_3 \end{pmatrix} = \begin{pmatrix} F_{thI} \\ F_{thII} \\ F_{thIII} \end{pmatrix}$$

where

$$(62) \quad \hat{Z} = \frac{1}{i\omega} \begin{pmatrix} m_1 D_{11} & m_1 D_{12} & m_1 D_{13} \\ m_2 D_{21} & m_2 D_{22} & m_2 D_{23} \\ m_3 D_{31} & m_3 D_{32} & m_3 D_{33} \end{pmatrix}$$

3.1. Add-on to the FDT approach

As already described in the section 1.3 once these matrices are found one can calculate the thermal noise of the i^{th} oscillator by applying the FDT [Callen] yielding, for the oscillator 2, to the equation

$$(63) \quad X_{th2}(\omega)^2 = \frac{4k_b T}{\omega^2} \Re\{(\hat{Z}(\omega)^{-1})_{22}\}$$

On the other hand, the generalized force correlation terms are related to the impedance matrix by the relations:

$$(64) \quad \hat{F}_{th}^2 = F_{gik}^2 = F_i F_k = 4k_b T \Re\{\hat{Z}_{ik}\} = \begin{pmatrix} F_{g11}^2 & F_{g12}^2 & F_{g13}^2 \\ F_{g21}^2 & F_{g22}^2 & F_{g23}^2 \\ F_{g31}^2 & F_{g32}^2 & F_{g33}^2 \end{pmatrix}$$

From the system (7) we can work out the explicit calculation of the displacement spectrum of the physical coordinate x_i in terms of the generalized force fluctuations. For the coordinate x_2 we get:


$$(65) \quad X_2 = D_{21}^{-1} \frac{F_{thI}}{m_1} + D_{22}^{-1} \frac{F_{thII}}{m_2} + D_{23}^{-1} \frac{F_{thIII}}{m_3}$$

And the computation of the displacement spectrum gives:

$$(66) \quad \begin{pmatrix} X_{th1}(\omega)^2 \\ X_{th2}(\omega)^2 \\ X_{th3}(\omega)^2 \end{pmatrix} = \hat{D}^{-1} \hat{F}_{th}^2$$

Then for the displacement spectrum of the coordinate X_2 is:

$$(67) \quad X_{th2}(\omega)^2 = D_{21}^{-1} \frac{F_{thI}}{m_1} + D_{22}^{-1} \frac{F_{thII}}{m_2} + D_{23}^{-1} \frac{F_{thIII}}{m_3}$$

	The thermal noise of the Virgo+ and Virgo Advanced Last Stage Suspension (The PPP effect).	DOC: Vir-015A-09 Issue: 1 Date: April 2009
---	---	--

Where

$$\begin{aligned}
D_{21}^{-1} &= \frac{1}{\det(D)} (D_{23}D_{31} - D_{21}D_{33}); \\
(68) \quad D_{22}^{-1} &= \frac{1}{\det(D)} (D_{11}D_{33} - D_{13}D_{31}); \\
D_{23}^{-1} &= \frac{1}{\det(D)} (D_{13}D_{21} - D_{11}D_{23});
\end{aligned}$$

And the computation of the displacement spectrum gives:

$$\begin{aligned}
(69) \quad X_{ihl}(\omega)^2 &= \left| D_{21}^{-1} \frac{F_{ihl}}{m_1} + D_{22}^{-1} \frac{F_{ihl}}{m_2} + D_{23}^{-1} \frac{F_{ihl}}{m_3} \right|^2 = \\
&= \frac{F_{g11}^2}{m_1^2} D_{21}^{-1} (D_{21}^{-1})^* + \frac{F_{g22}^2}{m_2^2} D_{22}^{-1} (D_{22}^{-1})^* + \frac{F_{g33}^2}{m_3^2} D_{23}^{-1} (D_{23}^{-1})^* + \\
&+ \frac{F_{g12}^2}{m_1 m_2} \left[D_{21}^{-1} (D_{22}^{-1})^* + D_{22}^{-1} (D_{21}^{-1})^* \right] + \frac{F_{g13}^2}{m_1 m_3} \left[D_{21}^{-1} (D_{23}^{-1})^* + D_{23}^{-1} (D_{21}^{-1})^* \right] + \frac{F_{g23}^2}{m_2 m_3} \left[D_{22}^{-1} (D_{23}^{-1})^* + D_{23}^{-1} (D_{22}^{-1})^* \right]
\end{aligned}$$

The predictions (69) and (63) are coincident, and this is due to the internal consistency of the FDT.

From the equation (69) we can learn the presence of a mixing term taking into account the effect of the correlation among the various generalized stochastic forces which suggests that in presence of two or more oscillators, the thermal noise cannot be calculated by a simple sum of the Brownian noises of the single oscillators.

This first conclusion can be better understood by studying the thermal noise with the normal mode approach.

3.2. The Normal Mode treatment

This kind of approach were already applied to the double oscillator system in the papers (Y. O. E. Majorana 1997) and (Rapagnani 1982).

The Lagrangian in (54) can be expressed as a sum of independent quadratic terms through the substitution of the new coordinates of the normal modes (y_+, y_o, y_-) related to (x_1, x_2, x_3) as follows:

$$(70) \quad \begin{pmatrix} Y_- \\ Y_o \\ Y_+ \end{pmatrix} = \hat{\Lambda}^{-1} \begin{pmatrix} X_1 \\ X_2 \\ X_3 \end{pmatrix}$$

where

$$(71) \quad \hat{\Lambda} = \begin{pmatrix} \lambda_{11} & \lambda_{12} & \lambda_{13} \\ \lambda_{21} & \lambda_{22} & \lambda_{23} \\ \lambda_{31} & \lambda_{32} & \lambda_{33} \end{pmatrix} = \begin{pmatrix} 1 & \frac{\omega_{03}^2 - \omega_0^2}{\omega_{03}^2} & 1 \\ \frac{\omega_{02}^2}{\omega_{02}^2 - \omega_-^2} & -\frac{\mu_{31}\omega_{03}^2}{\mu_{21}\omega_{02}^2} + \frac{\omega_{01}^2 + \mu_{21}\omega_{02}^2 + \mu_{31}\omega_{03}^2 - \omega_0^2}{\mu_{21}\omega_{02}^2} \left(1 - \frac{\omega_0^2}{\omega_{03}^2}\right) & -\frac{\omega_{02}^2}{\omega_{02}^2 - \omega_+^2} \\ \frac{\omega_{03}^2}{\omega_{03}^2 - \omega_-^2} & 1 & \frac{\omega_{03}^2}{\omega_{03}^2 - \omega_+^2} \end{pmatrix}$$

Hence we have:

$$(72) \quad \mathcal{L} = \frac{1}{2} m_- \dot{y}_-^2 + \frac{1}{2} m_o \dot{y}_o^2 + \frac{1}{2} m_+ \dot{y}_+^2 - \frac{1}{2} m_- \omega_-^2 y_-^2 - \frac{1}{2} m_o \omega_o^2 y_o^2 - \frac{1}{2} m_+ \omega_+^2 y_+^2$$

while the dissipation function of the system is:

$$(73) \quad E_{dn} = \frac{1}{2} m_+ \frac{\omega_+}{Q_+} \dot{y}_+^2 - \frac{1}{2} m_0 \frac{\omega_0}{Q_0} \dot{y}_0^2 - \frac{1}{2} m_- \frac{\omega_-}{Q_-} \dot{y}_-^2 + Cross(m_i, \omega_i, Q_i, \dot{y}_+ \dot{y}_-, \dot{y}_+ \dot{y}_0, \dot{y}_0 \dot{y}_-)$$

for some values of m_i, ω_i, Q_i ; $i = 1 \dots 3$ the term $Cross(m_i, \omega_i, Q_i, \dot{y}_+ \dot{y}_-, \dot{y}_+ \dot{y}_0, \dot{y}_0 \dot{y}_-)$ can be null and the diagonalization of the dissipative system is properly performed. It can be shown that the cross-term can be reduced to zero if :

$$(74) \quad \begin{aligned} Q_1 &= Q_3 \frac{\omega_1 (\omega_+^2 - \omega_3^2)(\omega_3^2 - \omega_-^2)}{\omega_2 (\mu_{31} \omega_3^4 - \mu_{21} \omega_2^4)} \\ Q_2 &= Q_3 \frac{\omega_2 (\omega_2^2 - \omega_-^2)(\omega_2^2 - \omega_+^2)}{\omega_3 (\omega_3^2 - \omega_-^2)(\omega_3^2 - \omega_+^2)} \end{aligned}$$

in this case the diagonalization of the dissipative system can be performed and the modes (y_+, y_0, y_-) can be properly called normal modes.

But, in general this is not true and (y_+, y_0, y_-) are called quasi-normal modes. In this approximation the normal modes treatment holds if the term $Cross(m_i, \omega_i, Q_i, \dot{y}_+ \dot{y}_-, \dot{y}_+ \dot{y}_0, \dot{y}_0 \dot{y}_-)$ remains negligible in the normal dissipation function (73).

Let us assume that the equations of the modes can be decoupled:

$$(75) \quad \begin{cases} \ddot{Y}_- + \frac{\omega_-}{Q_-} \dot{Y}_- + \omega_-^2 = \frac{F_{th-}}{m_-} \\ \ddot{Y}_0 + \frac{\omega_0}{Q_0} \dot{Y}_0 + \omega_0^2 = \frac{F_{th0}}{m_0} \\ \ddot{Y}_+ + \frac{\omega_+}{Q_+} \dot{Y}_+ + \omega_+^2 = \frac{F_{th+}}{m_+} \end{cases}$$

The quantities $\omega_-, \omega_0, \omega_+$ are the normal modes pulsations that can be calculated by the positive zeros of the real part of the matrix \hat{D} determinant, defined in equation (60) giving the equation:

$$(76) \quad \begin{aligned} \omega^6 + a_4 \omega^4 + a_2 \omega^2 + a_0 &= 0 \\ a_4 &= -(\omega_{01}^2 + (1 + \mu_{21}) \omega_{02}^2 + (1 + \mu_{31}) \omega_{03}^2) \\ a_2 &= \omega_{01}^2 (\omega_{02}^2 + \omega_{03}^2) + (1 + \mu_{21} + \mu_{31}) \omega_{02}^2 \omega_{03}^2 \\ a_0 &= -\omega_{01}^2 \omega_{02}^2 \omega_{03}^2 \end{aligned}$$

The normal masses m_-, m_0, m_+ are calculated by imposing the equivalence between the kinetic energy of the whole system in the espressions (54) and (72). We find:

$$(77) \quad \begin{pmatrix} m_- \\ m_0 \\ m_+ \end{pmatrix} = \begin{pmatrix} \lambda_{11}^2 & \lambda_{12}^2 & \lambda_{13}^2 \\ \lambda_{21}^2 & \lambda_{22}^2 & \lambda_{23}^2 \\ \lambda_{31}^2 & \lambda_{32}^2 & \lambda_{33}^2 \end{pmatrix} \begin{pmatrix} m_1 \\ m_2 \\ m_3 \end{pmatrix} = \hat{\Lambda}^2 \begin{pmatrix} m_1 \\ m_2 \\ m_3 \end{pmatrix}$$

The coupled quality factors can be found by imposing the equivalence between the dissipation function (73) in which we have replaced the relations (70) and the normal dissipation function (73). We notice that in general, there is a cross-term in the dissipation. We find:

$$\begin{aligned}
 Q_- &= \omega_- m_- \left[\frac{\omega_1 m_1}{Q_1} + \frac{\omega_2 m_2}{Q_2} \left(\frac{\omega_-^2}{\omega_-^2 - \omega_2^2} \right)^2 + \frac{\omega_3 m_3}{Q_3} \left(\frac{\omega_-^2}{\omega_-^2 - \omega_3^2} \right)^2 \right]^{-1} \\
 (78) \quad Q_+ &= \omega_+ m_+ \left[\frac{\omega_1 m_1}{Q_1} + \frac{\omega_2 m_2}{Q_2} \left(\frac{\omega_+^2}{\omega_+^2 - \omega_2^2} \right)^2 + \frac{\omega_3 m_3}{Q_3} \left(\frac{\omega_+^2}{\omega_+^2 - \omega_3^2} \right)^2 \right]^{-1} \\
 Q_0 &= \omega_0 m_0 \left[\frac{\omega_1 m_1}{Q_1} \left(1 - \frac{\omega_0^2}{\omega_3^2} \right)^2 + \frac{\omega_3 m_3}{Q_3} \frac{\omega_0^4}{\omega_3^4} - \frac{\omega_2 m_2}{Q_2} \left(\frac{\omega_1^2 \omega_3^2 + \omega_0^4 - \omega_0^2 (\omega_1^2 + (1 + \mu_{31}) \omega_3^2)}{\mu_{21} \omega_2^2 \omega_3^2} \right) \right]^{-1}
 \end{aligned}$$

The expressions of (78) are completely equivalent to those ones found in the reference (P. E. Majorana 1993). The normal forces are related to the generalized forces by the relations:

$$(79) \quad \begin{pmatrix} \frac{F_{th-}}{m_-} \\ \frac{F_{th0}}{m_0} \\ \frac{F_{th+}}{m_+} \end{pmatrix} = \hat{\Lambda}^{-1} \begin{pmatrix} \frac{F_{thI}}{M_1} \\ \frac{F_{thII}}{M_2} \\ \frac{F_{thIII}}{M_3} \end{pmatrix} \Rightarrow \begin{pmatrix} F_{th-} \\ F_{th0} \\ F_{th+} \end{pmatrix} = \hat{N} \begin{pmatrix} F_{thI} \\ F_{thII} \\ F_{thIII} \end{pmatrix}; \quad \hat{N} = \hat{M}_n \hat{\Lambda}^{-1} \hat{M}^{-1}$$

Applying the Langevin equation on the coordinate x_2 we find:

$$\begin{aligned}
 (80) \quad \langle X_{th2}(\omega)^2 \rangle &= \langle |\lambda_{21} Y_-(\omega) + \lambda_{22} Y_0(\omega) + \lambda_{23} Y_+(\omega)|^2 \rangle = \\
 &= \lambda_{21}^2 \langle |Y_-(\omega)|^2 \rangle + \lambda_{22}^2 \langle |Y_0(\omega)|^2 \rangle + \lambda_{23}^2 \langle |Y_+(\omega)|^2 \rangle + \\
 &+ \lambda_{21} \lambda_{22} \langle Y_-(\omega) Y_0^*(\omega) + Y_0(\omega) Y_-^*(\omega) \rangle + \\
 &+ \lambda_{21} \lambda_{23} \langle Y_-(\omega) Y_+^*(\omega) + Y_+(\omega) Y_-^*(\omega) \rangle + \\
 &+ \lambda_{22} \lambda_{23} \langle Y_0(\omega) Y_+^*(\omega) + Y_+(\omega) Y_0^*(\omega) \rangle
 \end{aligned}$$

taking into account the expressions (58) and the uncorrelation between the stochastic forces, we find:

$$(81) \quad \langle X_{th2}(\omega)^2 \rangle = \langle f_{th1}^2 \rangle |T_{n1}(\omega)|^2 + \langle f_{th2}^2 \rangle |T_{n2}(\omega)|^2 + \langle f_{th3}^2 \rangle |T_{n3}(\omega)|^2$$

where:

$$(82) \quad \begin{cases} T_{n1}(\omega) = N_{11}(\omega) \lambda_{21}(\omega) T_-(\omega) + N_{21}(\omega) \lambda_{22}(\omega) T_0(\omega) + N_{31}(\omega) \lambda_{23}(\omega) T_+(\omega) \\ T_{n2}(\omega) = (N_{12}(\omega) - N_{11}(\omega)) \lambda_{21}(\omega) T_-(\omega) + (N_{22}(\omega) - N_{21}(\omega)) \lambda_{22}(\omega) T_0(\omega) + (N_{32}(\omega) - N_{31}(\omega)) \lambda_{23}(\omega) T_+(\omega) \\ T_{n3}(\omega) = (N_{13}(\omega) - N_{11}(\omega)) \lambda_{21}(\omega) T_-(\omega) + (N_{23}(\omega) - N_{21}(\omega)) \lambda_{22}(\omega) T_0(\omega) + (N_{33}(\omega) - N_{31}(\omega)) \lambda_{23}(\omega) T_+(\omega) \end{cases} \text{and}$$

$$(83) \quad T_i(\omega) = \frac{1}{m_i} \frac{1}{\left(\omega^2 - \omega_i^2 + i \frac{\omega}{\tau_i} \right)}; \quad i = -, 0, +;$$

$$(84) \quad \langle f_{thi}^2 \rangle = \frac{k_b T m_i}{\tau_{0i}}; \quad i = 1, 2, 3$$

the relation (81) differs considerably by the naïve treatment of the thermal noise in which the calculation is performed by a simple quadratic sum of the thermal terms of the normal modes

$$(85) \quad \langle X_{th2}^{naive}(\omega)^2 \rangle = \lambda_{21}^2 |T_-(\omega)|^2 \langle F_{th-}^2 \rangle + \lambda_{22}^2 |T_0(\omega)|^2 \langle F_{th0}^2 \rangle + \lambda_{23}^2 |T_+(\omega)|^2 \langle F_{th+}^2 \rangle$$

The main difference is the presence is the equations (80)-(81) of the cross-term due to the correlation between the normal forces that in the equation (85) are erroneously neglected. In the condition in which the modes are orthogonal (the conditions (74) are satisfied) the cross-term is null and all the curves coincide. The stochastic cross-coupling is in this case identically zero. In the Figure 3-2 the general difference between naïve and the modal curves is shown.

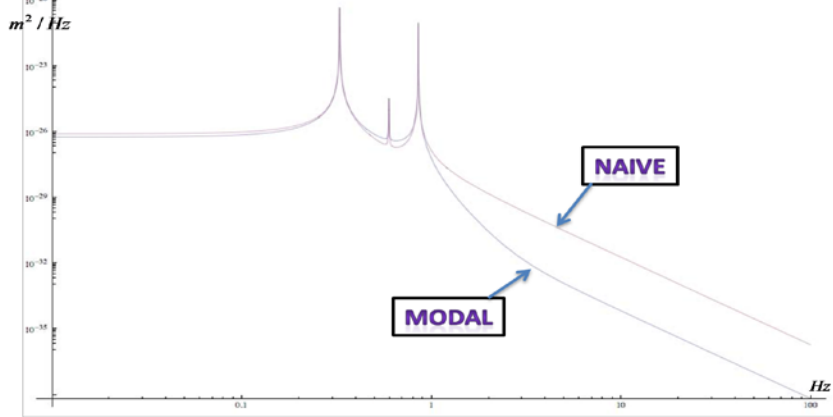


Figure 3-2 Thermal noise prediction of for the Virgo Branched pendulum calculated with the Normal Mode method, compared with the naïve calculation. We notice that the off-resonance zone at high frequencies is quite different, and in some cases, like ours, the cross-term give rise to a helpful cancellation, which reduces the thermal noise in the zone of the sensitivity.

3.3. The pendulum and the vertical modes.

The presented model can be used to calculate the thermal noise of the pendulum or the vertical modes by properly defining the elastic constants in the system. The following table will resumes the used definitions already introduced in section 1.1.

<p><i>Horizontal Modes (Pendulum)</i></p> $\omega_{p1}^2 = (\omega_{g1}^2 + \omega_{w1}^2) / \mu_t; \quad \mu_t = M_{mario} / M_T$ $\omega_{pi}^2 = \omega_{gi}^2 + \omega_{wi}^2; \quad i = 2, 3$ $\omega_{gi} = \sqrt{\frac{g}{L_i}} \quad \omega_{wi} = \sqrt{\frac{k_{el}^i}{m_i}}$ $k_{el}^i = \frac{n_i f_i \sqrt{\Lambda_i Y_i I_i^2}}{2L_i^2}; \quad I_2 = \frac{\pi}{4} r_{wi}^2$	<p><i>Vertical Modes</i></p> $\omega_{v1}^2 = (2\pi \cdot 0.4)^2 / \mu_t$ $\omega_{vi}^2 = \frac{\left(\frac{\pi r_{wi}^2 Y_i}{L_i} \right)}{m_i / 4}; \quad i = 2, 3$
--	---

where Y_i, r_{wi}, L_i are the Young modulus, the radius and the length of the suspension wires, while n_i, f_i the number of flexural points and the number of suspension wires of the i_{th} mass.

3.4. The structural and the viscous losses

In the model the losses of the system are defined by the mechanical quality factors of the oscillators. This is the most classical approach which comes from a very general treatise of the problem, and that can be found on classical texts like (Landau L.D. 1975) and in the papers like those of Callen and Greene (Greene F. 1952)(Callen H.B. 1952), in which the quality factor is related to the decay times of the uncoupled oscillators. The mechanical quality factors include both the structural and the viscous dissipation mechanisms that could be present on the suspension system by the relationships:

Pendulum modes $Q_1^{-1}(\omega) = \left(\Phi_1(\omega) \frac{\omega_1}{\omega} + Q_{vh1}^{-1} \right) / \sqrt{\mu_t};$ $Q_i^{-1}(\omega) = \left(\Phi_i(\omega) \frac{\omega_i}{\omega} + Q_{vhi}^{-1} \right); \quad i = 2, 3$	Vertical modes $Q_{iv}^{-1}(\omega) = \left(\Phi_{iv}(\omega) \frac{\omega_{iv}}{\omega} + Q_{vvi}^{-1} \right); \quad i = 1, 2, 3$
---	---

where Q_{vhi}, Q_{vvi} are the viscous quality factors and $\Phi_i(\omega), \Phi_{iv}(\omega)$ are the loss angles describing the structural losses of the suspension wires, and described in section 1.4.

4. Numerical Estimations

In the following several plots of the thermal noise estimations are shown. You'll find in the table below the parameters used for the computations.

Suspension wires Suspended element	Fused silica fibres Mirror	C85 wires Reference mass	Maraging wires Marionette
Suspended Mass	40 kg	40 kg	100 kg
N (number of wires)	4	4	1
Wire length	0.7m	0.7m	1.125m
Wire diameter	0.8mm	0.6mm	1.85mm
Young modulus	72GPa	200GPa	195GPa
Density	2200 kg/m ³	7900 kg/m ³	8000 kg/m ³
Specific heat	772 J/(kgK)	502 J/(kgK)	460 J/(kgK)
Thermal conductance	1.38	50	25
Thermal expansion	3.9 10 ⁻⁷ K ⁻¹	1.4 10 ⁻⁷ K ⁻¹	1.1 10 ⁻⁵ K ⁻¹
$\beta = 1/E dE/dTemp$	1.52 10 ⁻⁴ K ⁻¹	-2.782 10 ⁻⁴ K ⁻¹	-2.782 10 ⁻⁴ K ⁻¹
Internal ϕ	4.1 10 ⁻¹⁰	10 ⁻⁴	10 ⁻⁴
d_s	2.44 10 ⁻²	0	0
Horizontal viscous Q	-	10 ⁴	10 ³
Vertical viscous Q	-	10 ⁴	10 ³
θ_{H-V} Vert.-Hor. coupling		10 ⁻³	
Temp		290 K	
g		9.8 m/s ²	

Table 1: AdV parameters

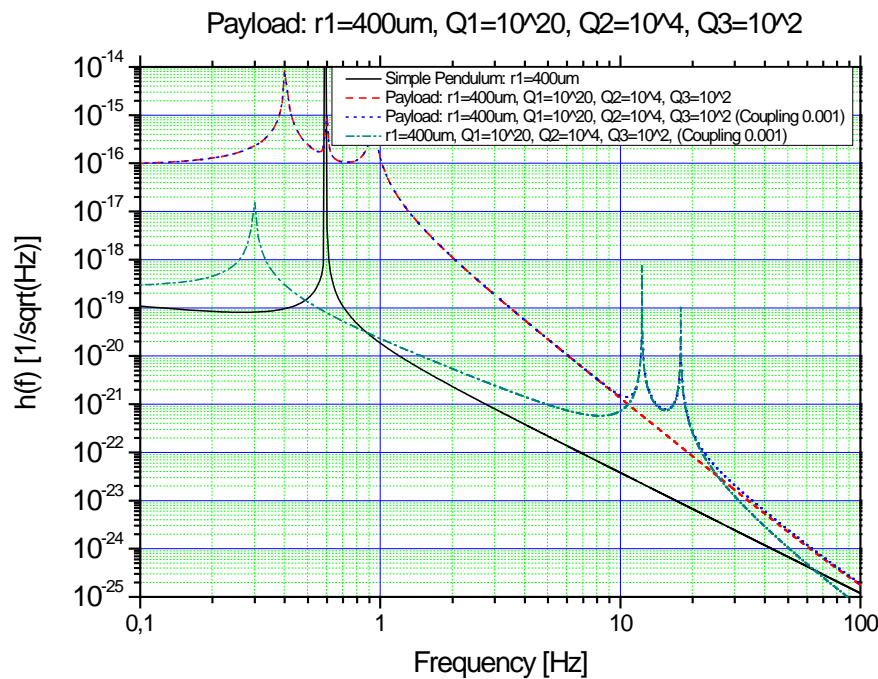


Figure 3- Thermal noise of the payload, compared with the simple pendulum if $Q_{\text{marionette}}=10^2$

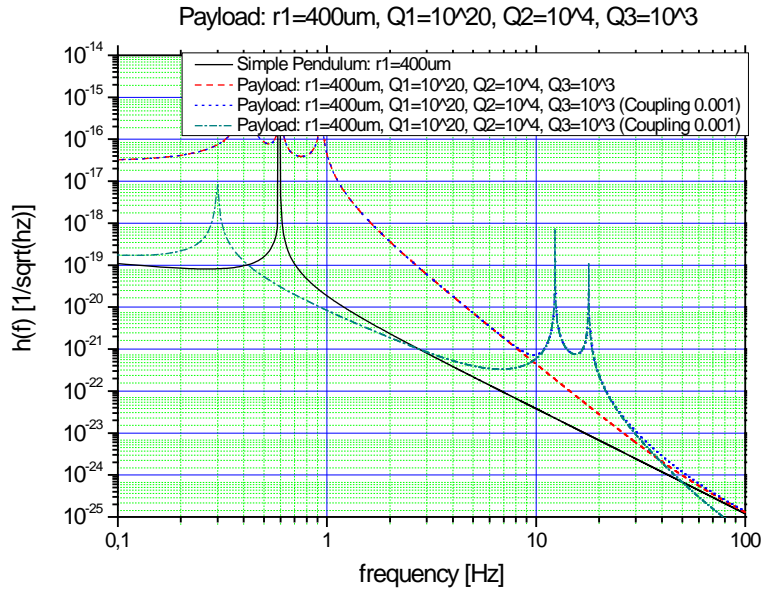
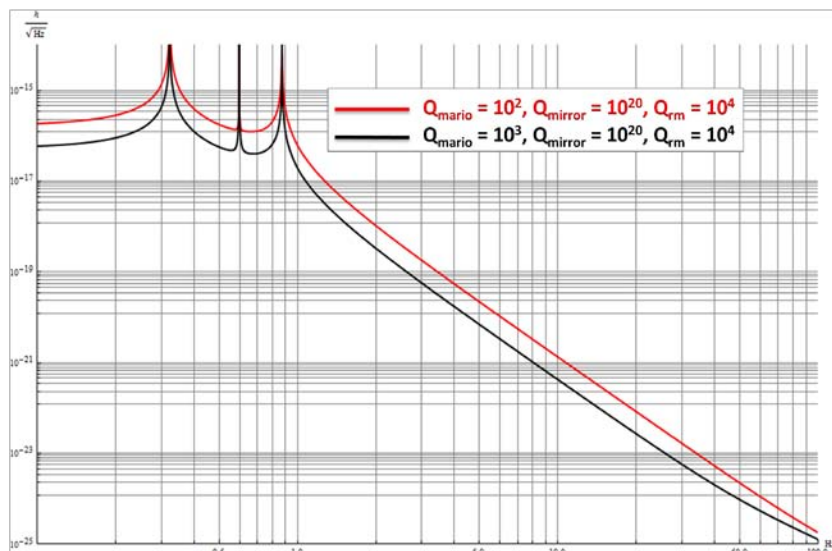


Figure 4 Thermal noise of the payload, compared with the simple pendulum if $Q_{\text{mario}}=10^3$

We have computed the thermal noise curves with the parameters of Virgo Advanced detector. We consider either the case in which the internal losses are dominant on the mirror losses, then the case in which the viscous damping is dominant. The parameters used are the same as in table Table 1.

4.1.1. Internal friction dominant

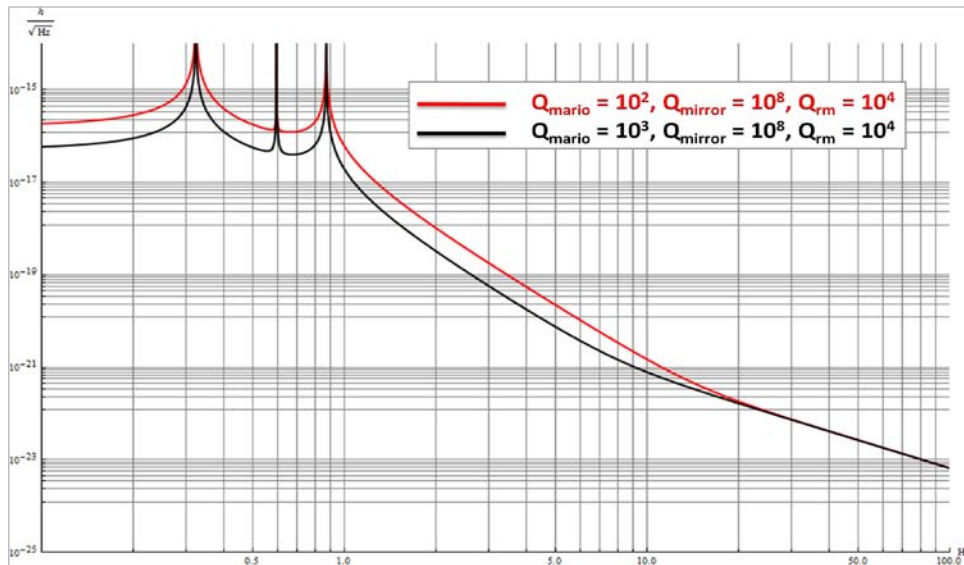
@10Hz	$\langle X_{th2}(\omega)^2 \rangle [m / \sqrt{Hz}]$	$\langle X_{pend}(\omega)^2 \rangle [m / \sqrt{Hz}]$	Ratio
$Q_{\text{mario}}=100$	2.66×10^{-18}	5.7×10^{-20}	46
$Q_{\text{mario}}=1000$	8.44×10^{-19}	5.7×10^{-20}	14



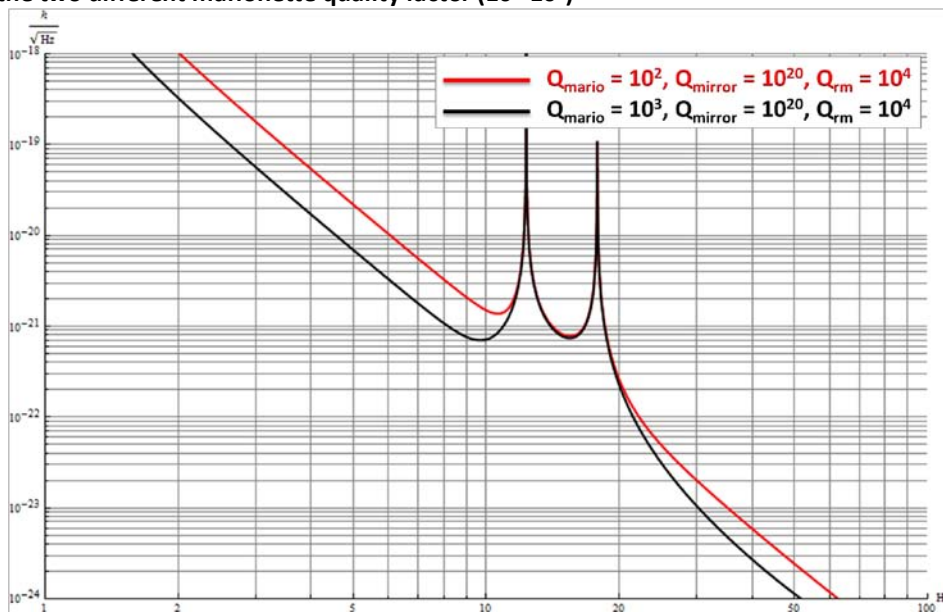
4-5 Pendulum Thermal noise in the case the viscous damping is negligible. The two cases correspond to the two different marionette quality factor (10^2 - 10^3)

4.1.2. Viscous Damping dominant

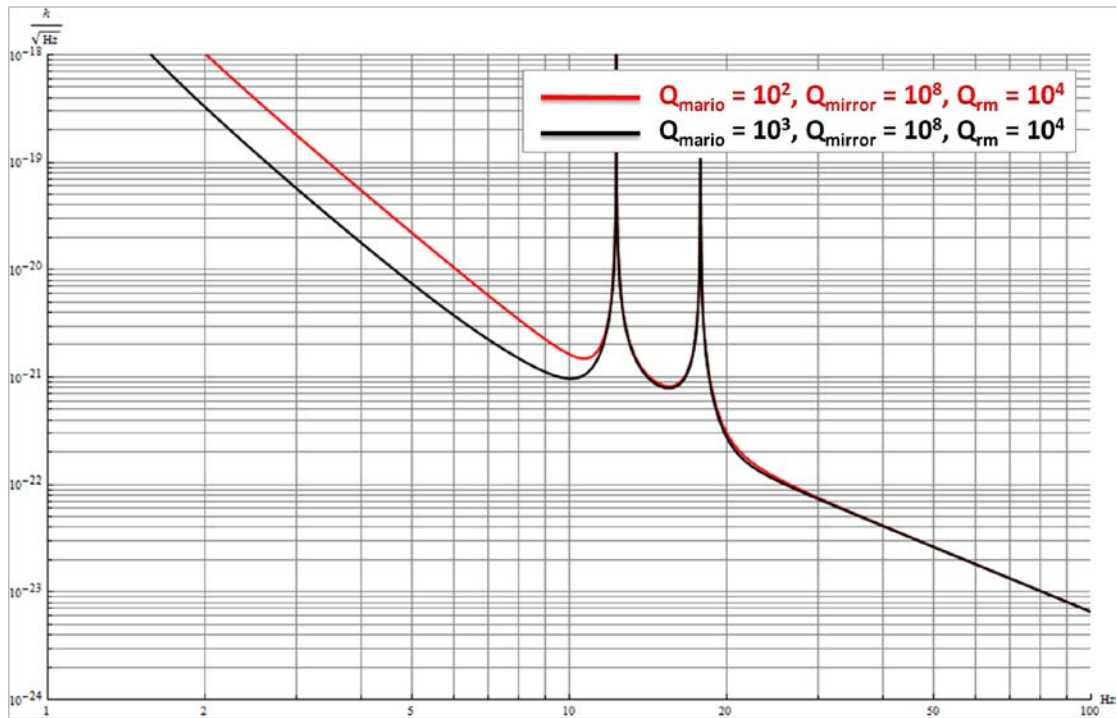
@10Hz	$\langle X_{th2}(\omega)^2 \rangle [m / \sqrt{Hz}]$	$\langle X_{pend}(\omega)^2 \rangle [m / \sqrt{Hz}]$	Ratio
$Q_{mario}=100$	2.84×10^{-18}	9.9×10^{-19}	2.9
$Q_{mario}=1000$	1.30×10^{-18}	9.9×10^{-19}	1.3



4-6 Pendulum Thermal noise in the case the viscous damping is comparable with the internal losses. The two cases correspond to the two different marionette quality factor (10^2 - 10^3)



4-7 Pendulum Thermal noise with vertical noise contribution in the case the viscous damping is negligible. The two cases correspond to the two different marionette quality factor (10^2 - 10^3)



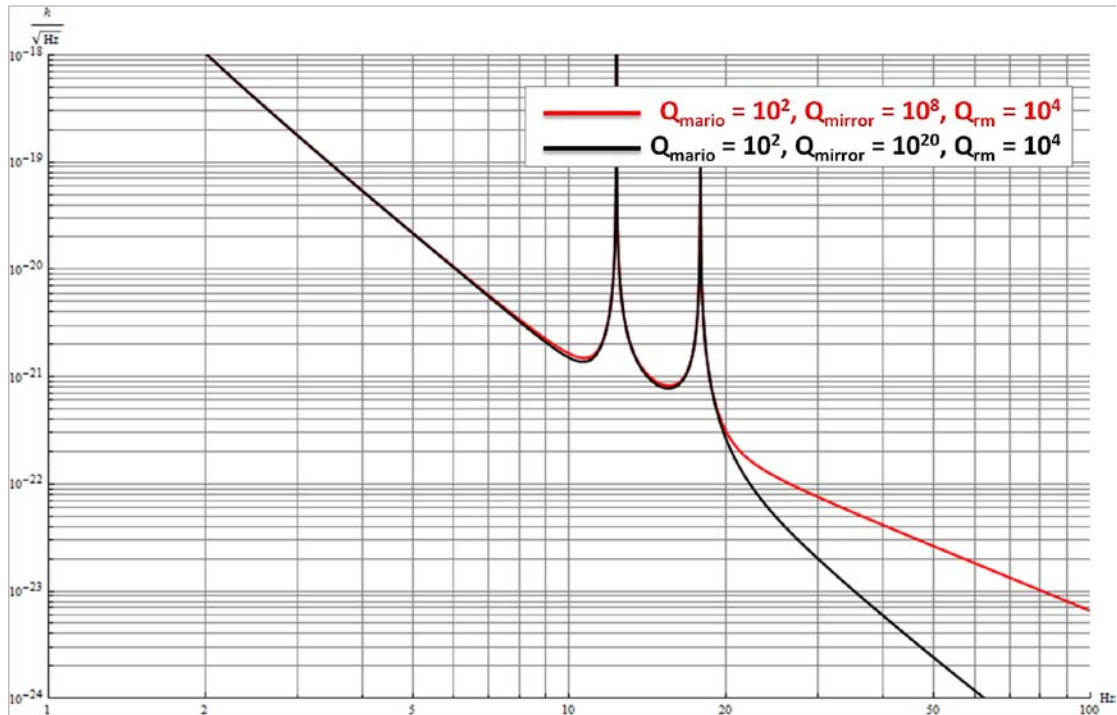
4-8 Pendulum Thermal noise in the case the viscous damping is comparable with internal losses. The two cases correspond to the two different marionette quality factor (10^2 - 10^3)

The overall curve gives quantitative results similar to what it has been illustrated in the previous paragraphs, but with the presence of the vertical thermal peeks.

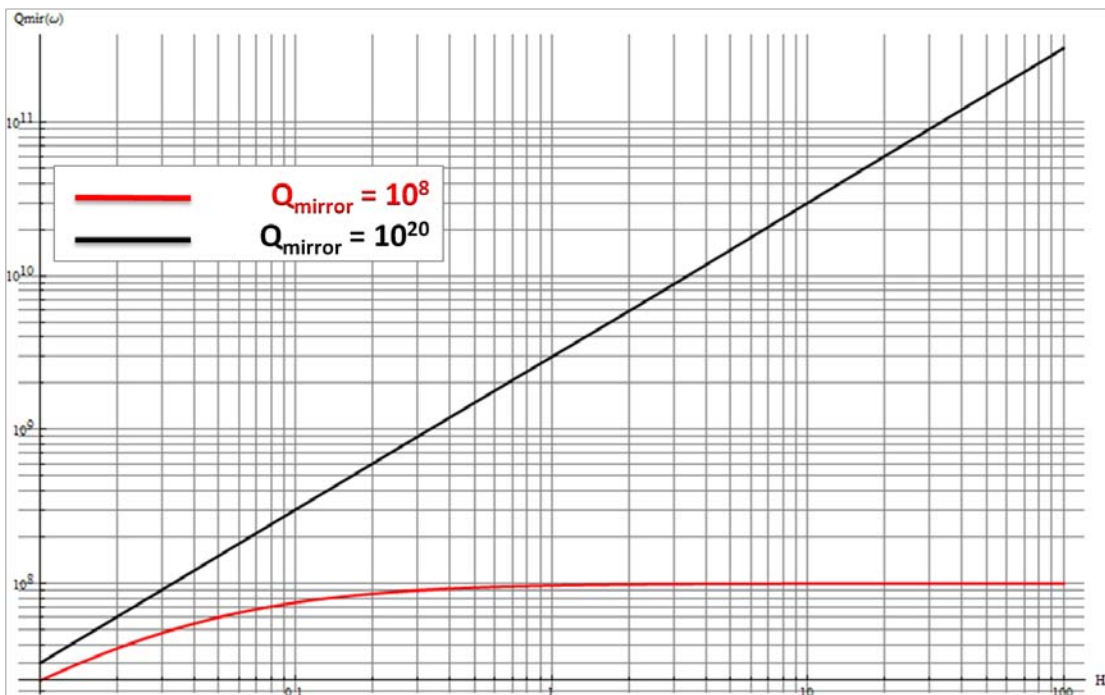
In figure 4-7 is shown a comparison between the overall thermal noise in the case the viscous losses on the mirror are negligible, and the case in which there is still viscous damping giving a quality factor of 10^8 on the mirror. The difference is evident in the off-resonance high frequency range by giving a change in the slope after 10 Hz related to the different frequency behavior in of the mirror quality factor as it is shown in figure 4-8.

The quality factors of the normal modes (at the resonances), for these two case are:

	$Q_{\text{mario}}=10^2$ - 10^3 , $Q_{\text{mirror}}=10^{20}$, $Q_{\text{rm}}=10000$	$Q_{\text{mario}}=10^2$ - 10^3 , $Q_{\text{mirror}}=10^8$, $Q_{\text{rm}}=10000$
Q_- ($\nu_-=0.40$ Hz)	180-1800	180-1800
Q_0 ($\nu_0=0.597$ Hz)	130000	130000
Q_+ ($\nu_+=0.937$ Hz)	150-1500	150-1500
Q_- vertical ($\nu_-=0.298$ Hz)	130-1300	130-1300
Q_0 vertical ($\nu_0=12.3$ Hz)	6800-36000	6800-36000
Q_+ vertical ($\nu_+=17.9$ Hz)	1000-1100	1000-1100



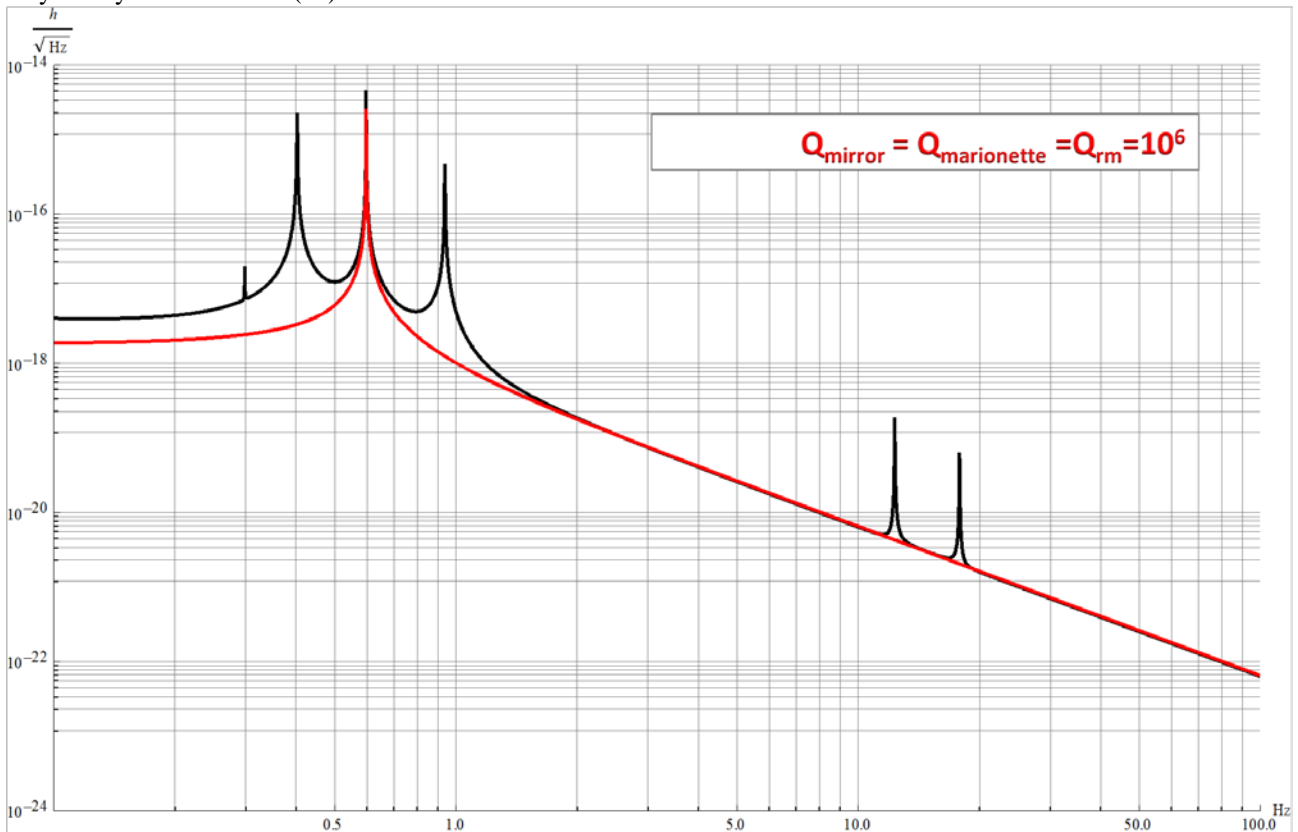
4-9 Comparison between the case in which an overall viscous damping is dominant (red curve) and the case in which the viscous damping on the suspension is negligible (black curve). The slope above 10 Hz is considerably different for the red curve.



4-10 Mirror pendulum quality factor vs frequency. Comparison between the cases with negligible viscous damping (black curve) and presence of a viscous damping (red curve). The change of slope in the red curve, explains the behavior of the thermal noise in the red curve of the figure 4-9.

4.1.3. The Normal condition.

In the following it is shown an example of the thermal noise in the normal case in which the uncoupled quality factors fully satisfy the conditions (74).



4-11 Thermal noise of the pendulum branched system compared with the simple pendulum in the normal mode condition (with vertical modes). The thermal noise of the branched suspension is identical to that one of the simple pendulum in the off-resonance high frequency zone (1: marionette, 2:mirror, 3: reaction mass). This is the ideal case in which all the quality factors are quite equal (to 10^6) and in the off-resonance high frequency zone the thermal noise of the branched suspension observed by the mirror coordinate, is identical to that one of the mirror one. This is consistent with the normal mode definition.

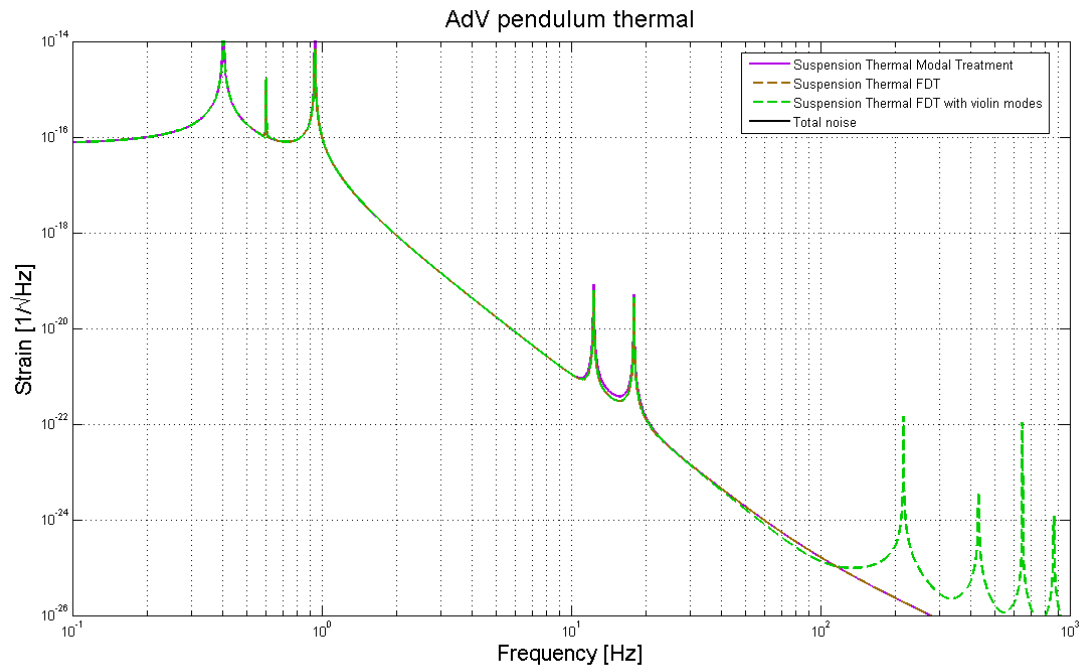


Figure 12 Comparison between the three models, the agreement is very good..

5. Conclusions I

In this paper we have calculated the thermal noise of the mirror last stage suspension which includes the marionette and the reaction mass. We have used three different approaches which lead all to the same results.

In the off-resonance high frequency region, the mechanical losses of the reaction mass and mainly of the marionette suspension can give non negligible contributions which induce the overall thermal noise curve to be different from the simple mirror curve even in the sensitivity bandwidth of the interferometer. This effect become more evident as soon as the mass of the mirror is more similar to that one of the marionette, and as soon as the mirror pendulum losses are further reduced. For these reasons the use of the overall thermal noise curve is crucial to give the correct evaluation of the design sensitivity of the Virgo+ and Virgo Advanced detectors in the low frequency regions of their bandwidth. Moreover this estimation can be helpful for the optimization of the last stage suspension design.



**The thermal noise of the Virgo+ and
Virgo Advanced Last Stage
Suspension (The PPP effect).**

DOC: Vir-015A-09

Issue: 1
Date: April 2009

6. On the quality factor of the marionette of the last stage suspension for the monolithic payload

From the results of the new calculation on the thermal noise of the last stage suspension, it turns out that the effect of the losses of the first oscillator in the branched chain can spoil the sensitivity of the interferometer.

As a consequence the evaluation of the losses of such an element, the marionette, is crucial for the correct evaluation of sensitivity curve.

The measurements we can deal with so far, come from a set of data taken on the payload hung to the SA. However these kind of measurements can be helpful to set a lower limit of the losses of the marionette, as it is influenced by the upper part of the SA chain.

Another set of measurement is performed on the last suspension system of the monolithic payload which are presently suspended in air, in the laboratory at 1500W.

6.1. The measurements

All these measurements give informations on the quality factors of the payload normal modes. Then, from these data we can yield the quality factors of the uncoupled oscillators by using the relationships calculated from the normal mode treatment.

6.1.1. On the SA chain

Set up			
$M_{\text{mirror}} = 21 \text{ kg}$	$L_{\text{mir}} = 0.7 \text{ m}$	$\phi_{\text{mir}} = 0.2 \text{ mm}$	Steel C85
$M_{\text{rm}} = 59 \text{ kg}$	$L_{\text{rm}} = 0.7 \text{ m}$	$\phi_{\text{rm}} = 0.6 \text{ mm}$	Steel C85
$M_{\text{mario}} = 110 \text{ kg}$	$L_{\text{mario}} = 1.125 \text{ m}$	$\phi_{\text{mario}} = 1.85 \text{ mm}$	Maraging Steel

	Meas Data		Freq. (Hz)		Calculated		Calculated
Q_{-}	50	v_{-}	0.446	Q_{mario}	30	Q_{-}	52
Q_0	$10^5-2 \cdot 10^6$	v_0	0.6	Q_{mirror}	10^5-10^7	Q_0	$10^5-1.8 \cdot 10^6$
Q_{+}	80	v_{+}	0.979	Q_{rm}	$>10^7$	Q_{+}	90
$Q_{- \text{ vert}}$		$v_{- \text{ vert}}$	0.3	Q_{mario}	30-50	$Q_{- \text{ vert}}$	
$Q_0 \text{ vert}$		$v_0 \text{ vert}$	4.17	Q_{mirror}	$>10^7$	$Q_0 \text{ vert}$	
$Q_{+ \text{ vert}}$	2000-3000	$v_{+ \text{ vert}}$	14.5	Q_{rm}	$>10^7$	$Q_{+ \text{ vert}}$	1936-3000

6.1.2. On the Virgo+ monolithic payload

Set up			
$M_{\text{mirror}} = 21 \text{ kg}$	$L_{\text{mir}} = 0.695 \text{ m}$	$\phi_{\text{mir}} = 0.285 \text{ mm}$	FS
$M_{\text{rm}} = 33 \text{ kg}$	$L_{\text{rm}} = 0.695 \text{ m}$	$\phi_{\text{rm}} = 0.6 \text{ mm}$	Steel C85
$M_{\text{mario}} = 115 \text{ kg}$	$L_{\text{mario}} = 1.130 \text{ m}$	$\phi_{\text{mario}} = 1.85 \text{ mm}$	Maraging Steel

	Meas Data		Frequencies		Calculated		Calculated
Q_{-}	600	v_{-}	0.421 Hz	Q_{mario}	1000	Q_{-}	500
Q_0	160	v_0	0.598 Hz	Q_{mirror}	200	Q_0	230
Q_{+}	220	v_{+}	0.842 Hz	Q_{rm}	300	Q_{+}	260
$Q_{- \text{ vert}}$	950	$v_{- \text{ vert}}$	5.316 Hz	Q_{mario}	900	$Q_{- \text{ vert}}$	960
$Q_0 \text{ vert}$	900	$v_0 \text{ vert}$	8.746 Hz	Q_{mirror}	1300	$Q_0 \text{ vert}$	900
$Q_{+ \text{ vert}}$	950	$v_{+ \text{ vert}}$	19.95 Hz	Q_{rm}	1500	$Q_{+ \text{ vert}}$	970



**The thermal noise of the Virgo+ and
Virgo Advanced Last Stage
Suspension (The PPP effect).**

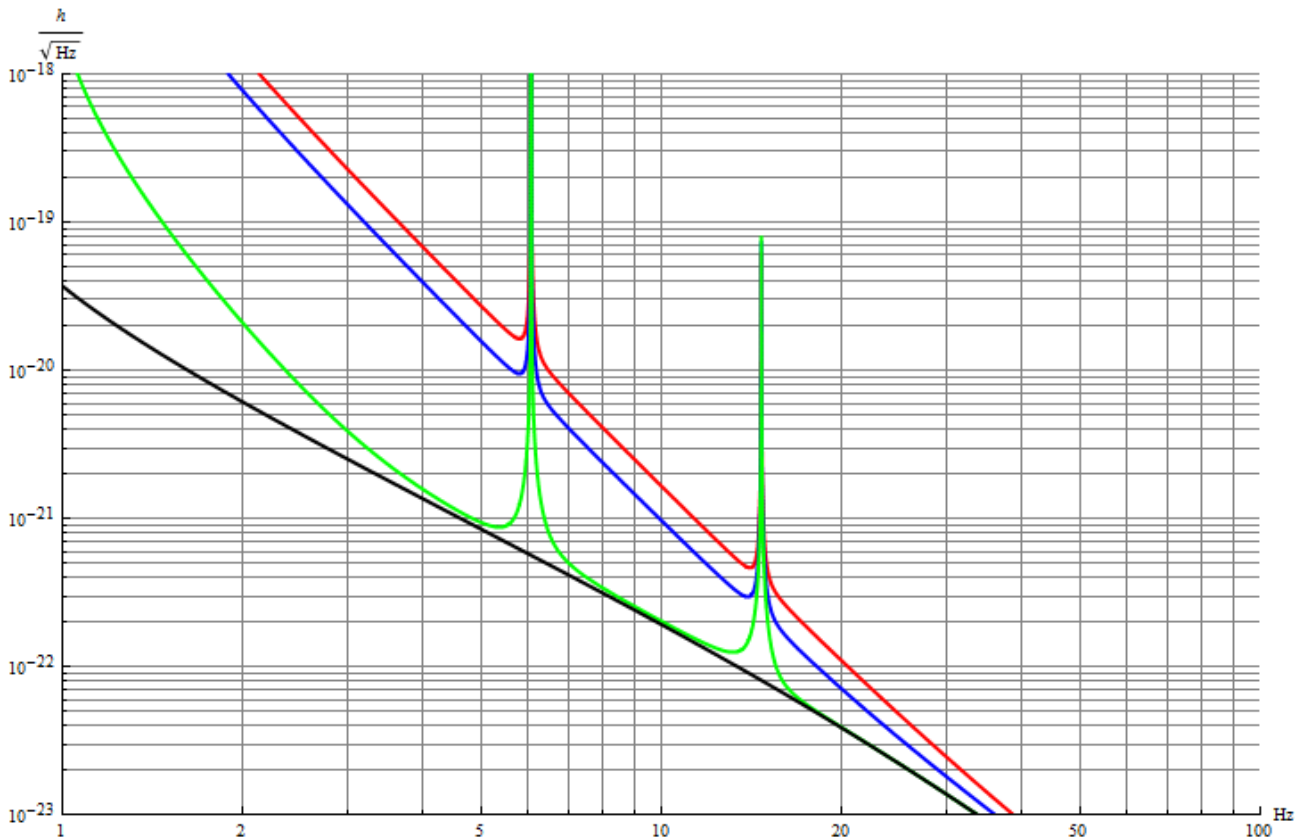
DOC: Vir-015A-09

Issue: 1
Date: April 2009

6.2. Conclusions II

From the measurements of the normal modes quality factors we can preliminarily set a lower limit to the marionette quality factor which is 1000. This factor, is measured on the monolithic suspension setup, in air and without the presence of the filter 7. The result suggests that it is possible to increase the quality factor of the marionette when it is mounted on the SA chain, by trying to improve its coupling to the filter 7, to be conservative we reckon that it is possible to improve by a factor 10 the losses by reaching a marionette quality factor of 300. Further investigations are needed for better understand this aspect. As a comparison, in figure Figure 12 we show the Virgo+ thermal noise with $Q_{\text{mario}}=1000, Q_{\text{rm}}>10^6$ (red) compared with $Q_{\text{mario}}=300, Q_{\text{rm}}>10^6$ (blue) and without viscous losses (green).

Suspension wires	Fused silica fibres	C85 wires	Maraging wires
Suspended element	Mirror	Reference mass	Marionette
Suspended Mass	20 kg	59 kg	110 kg
N (number of wires)	4	4	1
Wire length	0.7m	0.7m	1.125m
Wire diameter	0.285mm	0.6mm	1.85mm
Young modulus	72GPa	200GPa	195GPa
Density	2200 kg/m ³	7900 kg/m ³	8000 kg/m ³
Specific heat	772 J/(kgK)	502 J/(kgK)	460 J/(kgK)
Thermal conductance	1.38	50	25
Thermal expansion	3.9 10 ⁻⁷ K ⁻¹	1.4 10 ⁻⁷ K ⁻¹	1.1 10 ⁻⁵ K ⁻¹
$\beta = 1/E dE/dTemp$	1.52 10 ⁻⁴ K ⁻¹	-2.782 10 ⁻⁴ K ⁻¹	-2.782 10 ⁻⁴ K ⁻¹
Internal ϕ	4.1 10 ⁻¹⁰	10 ⁻⁴	10 ⁻⁴
d_s	2.44 10 ⁻²	0	0
Horizontal viscous Q	-	10 ⁴	10 ³
Vertical viscous Q	-	10 ⁴	10 ³
$\theta_{H,V}$ Vert.-Hor. coupling		10 ⁻³	
Temp		290 K	
g		9.8 m/s ²	




	The thermal noise of the Virgo+ and Virgo Advanced Last Stage Suspension (The PPP effect).	DOC: Vir-015A-09 Issue: 1 Date: April 2009
---	---	--

Figure 13 Virgo+ thermal noise with $Q_{\text{mario}}=1000$, $Q_{\text{rm}}>10^6$ (red) compared with $Q_{\text{mario}}=300$, $Q_{\text{rm}}>10^6$ (blue) and without viscous losses (green).

7. Bibliography

Bernardini A., Majorana E., Puppo P., Rapagnani P., Ricci F., Testi G. "Suspension last stages for the mirrors of the Virgo interferometric gravitational wave antenna." *Rev. Sci. Instr.* 70, no. 8 (1999): 3463.

Callen H.B., Greene F. «On a Theorem of Irreversible Thermodynamics I.» *Physical Review* 86, n. 5 (June 1952).

Goldstein, H. *Meccanica Classica*. Zanichelli .

Greene F., Callen H. B. «On a Theorem of Irreversible Thermodynamics. II.» (*Physical Review*) 88, n. 6 (December 1952).

Landau L.D., Lifshitz E.M. *Mechanics*. Mosca: Mir, 1975.

Majorana E., Ogawa Y. «Mechanical thermal noise in coupled oscillators.» *Physics Letters A* 233 (August 1997): 162-168.

Majorana E., Tricarico P. «Decay Times of an N-Normal Mode System.» *Il Nuovo Cimento* 108 B, n. 9 (September 1993): 1065.

Punturo M., Travasso F. *VIR-NOT-PER-1390-258*. Internal Note, Virgo, 2003.

Rapagnani, P. «Development and Test at T=4.2 K of a Capacitive Resonant Transducer for Cryogenic Gravitational Wave Antennas.» *Il Nuovo Cimento*, Luglio-Agosto 1982.